

HEATING THE HOT ATMOSPHERES OF GALAXY GROUPS AND CLUSTERS WITH CAVITIES: THE RELATIONSHIP BETWEEN JET POWER AND LOW-FREQUENCY RADIO EMISSION

E. O’SULLIVAN^{1,2}, S. GIACINTUCCI^{2,3,4}, L. P. DAVID², M. GITTI^{2,5}, J. M. VRTILEK², S. RAYCHAUDHURY¹ AND T. J. PONMAN¹

Draft version April 23, 2022

ABSTRACT

We present scaling relations between jet power and radio power measured using the Giant Metrewave Radio Telescope (GMRT), *Chandra* and *XMM-Newton*, for a sample of 9 galaxy groups combined with the Bîrzan et al. sample of clusters. Cavity power is used as a proxy for mechanical jet power. Radio power is measured at 235 MHz and 1.4 GHz, and the integrated 10 MHz–10 GHz radio luminosity is estimated from the GMRT 610–235 MHz spectral index. The use of consistently analysed, high resolution low-frequency radio data from a single observatory makes the radio powers for the groups more reliable than those used by previous studies, and the combined sample covers 6–7 decades in radio power and 5 decades in cavity power. We find a relation of the form $P_{\text{jet}} \propto L_{\text{radio}}^{\sim 0.7}$ for integrated radio luminosity, with a total scatter of $\sigma_{L_{\text{rad}}}=0.63$ and an intrinsic scatter of $\sigma_{i,L_{\text{rad}}}=0.59$. A similar relation is found for 235 MHz power, but a slightly flatter relation with greater scatter is found for 1.4 GHz power, suggesting that low-frequency or broad band radio measurements are superior jet power indicators. We find our low-frequency relations to be in good agreement with previous observational results. Comparison with jet models shows reasonable agreement, which may be improved if radio sources have a significant low-energy electron population. We consider possible factors which could bias our results or render them more uncertain, and find that correcting for such factors in those groups we are able to study in detail leads to a flattening of the $P_{\text{jet}}:L_{\text{radio}}$ relation.

Subject headings: galaxies: clusters: general — cooling flows — X-rays: galaxies: clusters — galaxies: active

1. INTRODUCTION

X-ray observations of clusters and groups over the past decade have provided strong evidence that, despite central cooling times significantly shorter than the Hubble time (e.g., Sanderson et al. 2006), relatively little gas actually cools below ~ 0.5 keV (Peterson et al. 2003; Kaastra et al. 2004). It is now widely accepted that active galactic nuclei (AGN) in the central dominant ellipticals of these systems can reheat the gas through a variety of mechanisms (Peterson & Fabian 2006; McNamara & Nulsen 2007, and references therein).

The most commonly observed evidence of interaction between AGN and the intra-cluster or intra-group medium (IGM) is the presence of cavities, formed when AGN jets inflate radio lobes, and identified from the resulting X-ray surface brightness decrement. Cavities provide a relatively simple method for estimating the power output of the jets, since the mechanical energy required to expel the IGM can be estimated from the cavity volume and surrounding pressure, and the timescale over which the cavity has formed can be estimated from dynamical arguments. Cavities are expected to heat the surrounding gas via the turbulent wake produced as they rise buoyantly through the IGM (Churazov et al. 2001). Studies of cavities have shown that the energies required to create them are sufficient to suppress cooling in systems across a wide range of mass scales (Bîrzan et al. 2004;

Dunn et al. 2005; Rafferty et al. 2006; Dunn et al. 2010).

The relationship between the mechanical power and radio emission of AGN jets and lobes is of interest for two main reasons: Firstly because it provides insight into the physical nature of the jet (e.g., Willott et al. 1999); Secondly because it allows estimation of the energy available from AGN based on more easily acquired radio data (e.g., Best et al. 2007). Bîrzan et al. (2004) determined the relation between cavity power and 1.4 GHz radio power, using a sample dominated by galaxy clusters. However, many cavities are undetected at 1.4 GHz since radiative aging will cause higher frequency emission to fade fastest once the jets cease to inject new plasma into the lobes. Bîrzan et al. (2008, hereafter B08) addressed the problem of these ghost cavities by measuring the relation at 327 MHz, and using an estimate of the integrated 10 MHz–10 GHz radio luminosity, both of which should be more reliable, and both of which produced steeper relations. Cavagnolo et al. (2010, hereafter C10) extended the relation to lower jet and radio powers by adding 21 giant ellipticals to the B08 sample, again finding a steeper slope, but were hampered by the poor quality of available archival low-frequency radio measurements.

We have compiled a sample of 18 galaxy groups, chosen to show signs of AGN/IGM interactions, and observed both by the Giant Metrewave Radio Telescope (GMRT) and by *Chandra* and/or *XMM-Newton* (Giacintucci et al. 2011, hereafter G11). Of these groups, nine have cavities (identified as decrements in surface brightness and in some cases as temperature or abundance features) which are clearly correlated with radio structures, and in this paper we add these to the B08 sample to examine the relations between jet mechanical power and radio power. Our sample has several advantages over previous studies: 1) Our low-frequency data were acquired from a single observatory and are analysed uniformly, making both flux density and spectral index measurements more reliable than

¹ School of Physics and Astronomy, University of Birmingham, Birmingham, B15 2TT, UK, email: ejos@star.sr.bham.ac.uk

² Harvard-Smithsonian Center for Astrophysics, 60 Garden Street, Cambridge, MA 02138, USA

³ INAF - Istituto di Radioastronomia, via Gobetti 101, I-40129, Bologna, Italy

⁴ Department of Astronomy, University of Maryland, College Park, MD 20742-2421, USA

⁵ Osservatorio Astronomico di Bologna - INAF, via Ranzani 1, I-40127, Bologna, Italy

is possible for data collected from mixed archival sources; 2) We are able, for the first time, to measure the integrated radio luminosity for a significant number of low-radio-luminosity systems, as well as single-frequency powers; 3) We have a closer correlation between radio and X-ray morphologies in most cases, than is possible either at 1.4 GHz (where many cavities are undetected) or with low-resolution low-frequency observations (where unrelated sources may be difficult to remove); 4) Our groups have low radio and cavity powers (typically $P_{\text{cav}} \lesssim 10^{44} \text{ erg s}^{-1}$ and $P_{1400} \lesssim 10^{24} \text{ W Hz}^{-1}$), filling in a region of parameter space sparsely populated in the B08 sample.

We describe our sample and analysis techniques in §2. Our results and their relation to previous work are discussed in §3, and we present our conclusions in §4. A Λ CDM cosmology with $H_0=70 \text{ km s}^{-1} \text{ Mpc}^{-1}$ and $\Omega_M=1-\Omega_\Lambda=0.3$ is adopted throughout the paper. The radio spectral index α is defined as $S_\nu \propto \nu^{-\alpha}$, where S_ν is the flux density at frequency ν .

2. OBSERVATIONS AND DATA ANALYSIS

The nine groups in our study were selected to have cavities and X-ray data of sufficient quality to allow a reliable determination of the properties of the IGM. Table 1 lists the properties of the sample. Images and an in-depth description of the radio properties of the groups are presented in G11. We do not include the giant sources NGC 315, NGC 383 and NGC 7626, since the available data do not allow clear identification of cavities. NGC 315 and NGC 383 extend outside the *XMM* field of view, and NGC 7626 is in a merging group (Randall et al. 2009) where determination of IGM properties and gravitating mass is unreliable. NGC 1407 is not included since the cavity tentatively identified by Dong et al. (2010) is on a much smaller scale than the radio emission, and its identification and size vary with image processing. NGC 741, where a ghost cavity has been previously identified (Jetha et al. 2008) is excluded since the visible radio emission appears to be unrelated to the cavity, and is contaminated by a second AGN within the group. UGC 408 was not listed as a cavity system in G11, as no detailed examination of its structure has yet been published. However, it is included in this sample, since its radio source appears to have cleared an elliptical cavity in the group centre; it was also included in the C10 sample. A more detailed description of IGM structures in our full sample of 18 groups will be presented in a later paper.

In three cases we had already published individual studies of the cavities; AWM 4 (O’Sullivan et al. 2010), HCG 62 (Gitti et al. 2010) and NGC 5044 (David et al. 2009). For these groups, we used the gas properties determined from these prior analyses. We note that for HCG 62 the gas temperature and density profiles were extracted from an *XMM-Newton* observation; in all other cases *Chandra* data were used.

For the remaining systems, we determined the gas properties from the longest available *Chandra* observations. Table 1 provides basic information on each dataset. Observations were downloaded from the *Chandra* archive and reprocessed using CIAO 4.2 and CALDB 4.3.0 following the standard techniques described in the *Chandra* analysis threads⁶ and O’Sullivan et al. (2010). Point sources were identified using the WAVDETECT task and, with the exception of sources coincident with the group-central AGN, removed. As the groups typically fill the field of view, background spectra were

drawn from the standard set of ACIS blank sky background events files, scaled to produce the same 9.5–12.0 keV count rate as that in the target observation. Very faint mode screening was applied to target and background observations where appropriate.

Spectra were extracted from circular annuli and a deprojected absorbed APEC model (Smith et al. 2001) was fitted to each set of spectra using XSPEC v12.6.0k. The absorbing column was fixed at the galactic value determined from the survey of Kalberla et al. (2005). Redshifts and adopted distances for each group are given in G11. Energies below 0.5 keV and above 7 keV were ignored during fitting, so as to minimise calibration and background uncertainties.

Jet powers were assessed using the standard approach of assuming that the mechanical power of the jet can be approximated as the energy of the detected cavities averaged over some timescale (e.g., Birzan et al. 2004, B08). We define the energy of each cavity to be $4pV$, the enthalpy of a cavity filled with a relativistic plasma. Cavity sizes are defined by matching an ellipse to their apparent shape, and assuming a line-of-sight depth equal to the minor axis. Uncertainties on the volume are estimated by assuming a minimum depth of half this value, and a maximum equal to the major axis. The uncertainty on the volume is, in most cases, the largest contributor to the uncertainty on the energy of each cavity and the total uncertainty on the cavity power. Outburst timescales are typically estimated from the buoyant rise time of the cavities (t_{buoy} , Churazov et al. 2001), but we also estimate the sonic timescale (i.e., the travel time between the AGN and farthest point of the cavity at the sound speed) and refill timescale of the cavities. Our cavity power estimates assume the buoyancy timescale, to ensure that they are directly comparable with previous studies. The uncertainty on this estimate includes the uncertainties on volume, pressure, and t_{buoy} . These values are used when fitting the relations between cavity power and radio power. The additional uncertainty associated with the other timescale estimates is indicated when we plot these relations, but is not included in the fitting process.

The analysis of our GMRT radio data is described in G11. Most of the groups in the sample were observed at both 235 MHz and 610 MHz, but of the cavity systems included in this study, NGC 5813 was only observed at 235 MHz and NGC 5846 only at 610 MHz. Radio powers at each frequency, P_ν , are estimated as $P_\nu=4\pi D_L^2(1+z)^{\alpha-1}S_\nu$, where S_ν is the flux density at frequency ν , α the spectral index, z is the redshift and D_L is the luminosity distance to the source. Radio powers at 1.4 GHz were also estimated from flux densities mainly derived from the NRAO VLA Sky Survey (NVSS, Condon et al. 1998).

Since it is desirable to compare our 235 MHz GMRT measurements with the 327 MHz VLA radio powers used by B08, we have used the spectral indices given in B08 and G11 to correct each set of flux densities to the other band, and determined the best-fitting relationship between cavity power and radio power for both frequencies. It should be noted that while G11 determined 235–610 MHz spectral indices for the majority of their sample, only a lower limit on the spectral index could be determined for NGC 5044 ($\alpha > 1.9$), and no index could be determined for NGC 5813 or NGC 5846, since they were only observed at one frequency. When correcting those data to 327 MHz, we adopt a spectral index of $\alpha=1.9$ for NGC 5044, the 235 MHz–1.4 GHz spectral index, $\alpha=0.94$, for NGC 5813, and the 610 MHz–1.4 GHz spectral

⁶ <http://asc.harvard.edu/ciao/threads/index.html>

Table 1
Summary of observations and data for each group

Group	Instrument	ObsID	t_{exp} (ks)	D (Mpc)	α_{235}^{610}	P_{1400} (10^{24} W Hz $^{-1}$)	P_{235} (10^{24} W Hz $^{-1}$)	L_{radio} (10^{42} erg s $^{-1}$)	P_{cav}^d (10^{42} erg s $^{-1}$)
AWM 4	ACIS-S	9423	74.5	128.7	0.67	1.41 ± 0.07	6.31 ± 0.50	0.14 ± 0.02	$53.62^{+29.35}_{-9.05}$
HCG 62	ACIS-S	10462	67.1	57.8	1.15	0.0021 ± 0.0001	0.018 ± 0.001	0.00029 ± 0.00003	$3.49^{+0.91}_{-1.66}$
	XMM	050478501	122.5	-	-	-	-	-	-
UGC 408	ACIS-S	11389	93.9	61.9	0.53	0.83 ± 0.04	2.57 ± 0.21	0.071 ± 0.008	$3.53^{+2.69}_{-2.75}$
NGC 507	ACIS-I	2882	43.5	69.3	1.14	0.060 ± 0.003	0.68 ± 0.05	0.011 ± 0.001	$20.68^{+28.72}_{-5.58}$
NGC 4636	ACIS-I	3926	74.6	13.2	0.61	0.0017 ± 0.0001	0.0053 ± 0.0004	0.00013 ± 0.00002	$0.28^{+0.11}_{-0.04}$
NGC 5044	ACIS-S	9399	82.7	38.2	$> 1.90^a$	0.0065 ± 0.0003	0.042 ± 0.003	0.0019 ± 0.0002	$2.88^{+2.55}_{-0.45}$
NGC 5813	ACIS-S	9517	98.8	26.8	0.94^b	0.0014 ± 0.0001	0.0079 ± 0.0006	0.00013 ± 0.00002	$1.64^{+0.29}_{-0.20}$
NGC 5846	ACIS-I	7923	90.0	24.3	0.65^c	0.0015 ± 0.0001	-	0.00011 ± 0.00001	$1.71^{+0.50}_{-0.44}$
NGC 6269	ACIS-I	4972	39.6	142.9	0.73	0.141 ± 0.007	0.65 ± 0.05	0.013 ± 0.002	$10.02^{+2.20}_{-2.80}$

Note. — ^a Only a lower limit on the 235-610 MHz spectral index, α_{235}^{610} , could be estimated for NGC 5044, as extended structures at 235 MHz are undetected at higher frequencies (see G11). ^b NGC 5813 spectral index measured between 235 MHz and 1.4 GHz. ^c NGC 5846 spectral index measured between 610 MHz and 1.4 GHz. ^d Cavity power estimated based on the buoyancy timescale and including uncertainties on volume, pressure, and timescale.

index, $\alpha=0.65$, for NGC 5846.

We also estimate the integrated radio luminosity of our groups in the 10 MHz-10 GHz band, assuming a powerlaw spectrum and using the same spectral indices. These are not perfectly comparable with the integrated radio power estimates of Bîrzan et al., which are based on model fits to flux densities measured at 3-8 frequencies for each system. However, the inaccuracy introduced by our use of a simple spectral index is unlikely to be significant compared to the large uncertainties in cavity power. Low-frequency spectral index measurements such as ours should not be strongly affected by radiative losses unless the break frequency is below our lowest measurement frequency (235 MHz). It seems unlikely that any of our systems are so old. Two groups in the sample, NGC 507 and AWM 4, have unusually high radiative age estimates (Murgia et al. 2011; Giacintucci et al. 2008) but break frequencies of 300-450 MHz, above our lower frequency bound. If the spectral indices are accurate, then we are unlikely to over-estimate the steepness of the spectrum and the power at low frequencies, as would probably be the case if high-frequency spectral indices were used. Detailed modelling of the radio spectra for our group sample and revised estimates of integrated radio power will be presented in a forthcoming paper.

3. RESULTS AND DISCUSSION

Figure 1 shows cavity power vs. radio power at 1.4 GHz and 235 MHz for our nine groups and the 24 systems described by B08. At both frequencies, the scatter among the points is considerable. The effect of radiative aging on the radio sources causes preferential fading of emission at higher frequencies. We therefore expect the low-frequency measurements to provide a more accurate estimate of the true radio power in older systems. Figure 2 shows the relationship between cavity power and the integrated radio luminosity in the 10 MHz-10 GHz band. The integrated luminosity should be a superior measure of the radiative power compared to estimates at a single frequency, since it accounts for variations in spectral index between sources. However, we still see a large degree of scatter amongst the data points.

We used the bivariate correlated error and intrinsic scatter (BCES) algorithm (Akritas & Bershady 1996) to perform linear regression fits to the data, determining the best fitting

power-law relationship between cavity power, P_{cav} , and the radio powers at each frequency (P_{1400} , P_{235} , P_{327}) or the integrated radio luminosity L_{radio} . Using the orthogonal BCES regression to the parameters in log space, the best-fit relations are:

$$\log P_{\text{cav}} = 0.71 (\pm 0.11) \log P_{235} + 1.26 (\pm 0.12) \quad (1)$$

$$\log P_{\text{cav}} = 0.72 (\pm 0.11) \log P_{327} + 1.38 (\pm 0.12) \quad (2)$$

$$\log P_{\text{cav}} = 0.63 (\pm 0.10) \log P_{1400} + 1.76 (\pm 0.15) \quad (3)$$

$$\log P_{\text{cav}} = 0.71 (\pm 0.11) \log L_{\text{radio}} + 2.54 (\pm 0.21) \quad (4)$$

where P_{cav} and L_{radio} are in units of 10^{42} erg s $^{-1}$, and P_{235} , P_{327} and P_{1400} in units of 10^{24} W Hz $^{-1}$.

We estimated the total scatter in the data using the technique described in Pratt et al. (2009), which is based on weighted estimates of the orthogonal distance between the data points and best fit lines. We find the total scatter for the radio power relations to be $\sigma_{1400}=0.68$ dex and $\sigma_{235}=0.62$ dex, while the integrated radio luminosity relation has a scatter of $\sigma_{L_{\text{rad}}}=0.63$. The intrinsic scatter in the data can be estimated by subtracting the contribution expected from the statistical errors. We found that the scatter about the radio power relations was $\sigma_{i,1400}=0.65$ dex and $\sigma_{i,235}=0.58$ dex, and the scatter about the integrated radio luminosity relation was $\sigma_{i,L_{\text{rad}}}=0.59$ dex.

These relations can be compared with those derived by B08, including the correction to the 327 MHz relation given by Bîrzan et al. (2010) and using the integrated radio luminosity from their sources as a whole rather than from the lobes alone:

$$\log P_{\text{cav}} = 0.51 (\pm 0.07) \log P_{327} + 1.51 (\pm 0.12) \quad (5)$$

$$\log P_{\text{cav}} = 0.35 (\pm 0.07) \log P_{1400} + 1.85 (\pm 0.10) \quad (6)$$

$$\log P_{\text{cav}} = 0.49 (\pm 0.07) \log L_{\text{radio}} + 2.32 (\pm 0.09) \quad (7)$$

However, these relations were estimated using an ordinary least-squares regression, minimising the distance between fit line and data points in the P_{cav} axis only. Refitting these relations using the orthogonal BCES regression steepens them and increases the uncertainties, giving slopes of 0.67 ± 0.19 at 327 MHz, 0.57 ± 0.17 at 1.4 GHz and 0.68 ± 0.19 for the integrated radio power. HCG 62, the only group in the B08

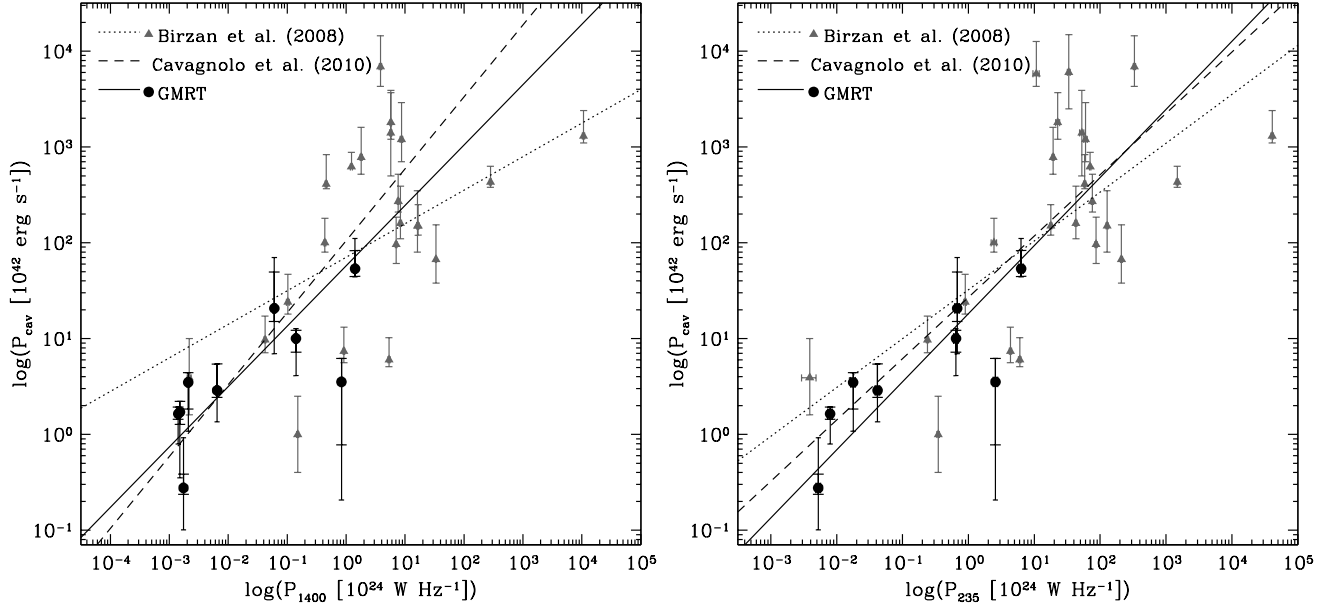


Figure 1. Cavity power vs. radio power at 1.4 GHz (left) and 235 MHz (right). Systems in the sample of B08 are marked by grey triangles, members of our groups sample by black circles. 1σ uncertainties on radio power and cavity power (calculated using the buoyant rise time of the cavities) are indicated by error bars. In many cases the uncertainty on the radio luminosity is smaller than the data point. For our groups, additional narrow-width error bars indicate the 1σ uncertainty range allowing for alternate measures of cavity age (the sonic and refill timescales). The Birzan et al. point with the lowest radio power is HCG 62, which is also included in our GMRT groups sample. This point is included for comparison, but was excluded from our analysis. The solid fit line indicates our BCES regression fit to the data points. The dotted line indicates the relation found by B08, the dashed line the relation found by C10. For the 235 MHz relation, we have used the spectral indices given by B08 to correct their 327 MHz data to 235 MHz, so as to allow a direct comparison with our data. The normalizations of the Birzan or Cavagnolo fit lines are not corrected for frequency differences, but the lines are indicative of the relative gradient of the different fits.

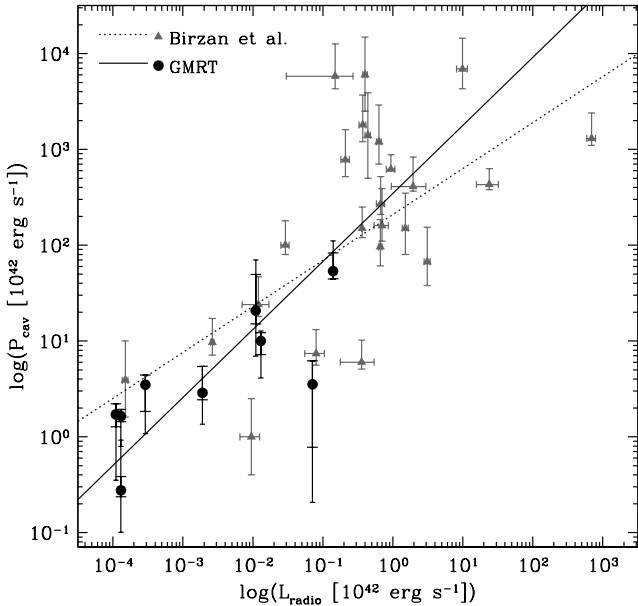


Figure 2. Cavity power vs. integrated 10 MHz-10 GHz radio power. Symbols are the same as in Fig. 1.

sample, has a strong influence. Excluding this system, fits to the B08 dataset have gradients of 0.81 ± 0.30 at 327 MHz, 0.62 ± 0.28 at 1.4 GHz, and 0.78 ± 0.30 for the integrated radio power. This steepening, and the large uncertainties on the gradients, emphasize the need for a large dynamic range if gradients are to be measured accurately from data with such a large degree of scatter.

B08 also found steeper relations when fitting only those systems where the radio emission fills the cavities seen in the X-ray, excluding systems with ghost cavities. A comparison of radio and cavity power on this basis is likely to be more reliable, since the radio emission is clearly associated with the lobes which inflated the cavity. Our relations have gradients which are steeper than the published B08 relations (though consistent with them at the 1.6 - 2.3σ significance level), and in agreement with those derived from the Birzan et al. sample using orthogonal regression. The total scatter about the B08 radio luminosity relation is $\simeq 0.83$ dex, suggesting that our groups are more closely clustered about the relation.

Cavagnolo et al. (2010), using orthogonal BCES regression, found the following relations between radio power and cavity power:

$$\log P_{\text{cav}} = 0.64 (\pm 0.09) \log P_{200-400} + 1.54 (\pm 0.12) \quad (8)$$

$$\log P_{\text{cav}} = 0.75 (\pm 0.14) \log P_{1400} + 1.91 (\pm 0.18) \quad (9)$$

Unsurprisingly, given the large overlap between our sample and that of C10 (The C10 sample of 21 ellipticals includes 8 of our 9 groups, and both sets of fits have the B08 sample in common) their best-fitting relations are very similar to those we derive, with gradients in agreement to within the 1σ uncertainties at both 1.4 GHz and at lower frequencies. C10 drew their low frequency radio measurements from the CATS database (Verkhodanov et al. 1997), a compilation of data from numerous radio catalogues. We expect there to be significant variations in sensitivity and resolution among measurements from different observatories and surveys. Our GMRT 235 MHz were observed and processed uniformly, and we therefore expect our data points to be more reliable. Comparison of our 235 MHz radio powers with the 200-400 MHz

powers of C10 suggests that agreement is fairly good for the most radio luminous systems ($P_{235} \gtrsim 10^{23} \text{ W Hz}^{-1}$). However, for the fainter sources, disagreements of a factor of ~ 10 are typical. This may be explained by issues such as the inclusion of unresolved background sources and the non-detection of faint structures. The total scatter about the C10 relations is comparable with ours at low frequencies ($\sigma_{200-400}=0.61$) and slightly larger at 1.4 GHz ($\sigma_{1400}=0.78$).

3.1. Comparison with theoretical models

Willott et al. (1999) determined a theoretical relation between radio luminosity and jet power which is now widely used to estimate the kinetic energy output of AGN (e.g., Hardcastle et al. 2007; Cattaneo & Best 2009). This model takes the form

$$P_{\text{jet}} = 3 \times 10^{38} f^{3/2} P_{151}^{6/7} \text{ W}, \quad (10)$$

where P_{jet} is the total jet power, P_{151} is its observed 151 MHz radio power in units of $10^{28} \text{ W Hz}^{-1} \text{ Sr}^{-1}$, and the factor f includes a variety of unknown factors affecting the normalisation of the relation. Under the assumption that the spectra of radio sources are simple powerlaws, the normalisation of the model is dependent on frequency, but its gradient is not. Since P_{cav} is a proxy for the total jet power, it is straightforward to compare the model gradient with those of measured $P_{\text{cav}}:P_{\text{radio}}$ relations. C10 compared their best fitting $P_{\text{cav}}:P_{1400}$ relation with the model, finding that its gradient of ~ 0.86 agreed with their measured gradient within errors. At lower frequencies, which should be more reliable, the model agrees with the C10 $P_{\text{cav}}:P_{200-400}$ relation within $\sim 2.5\sigma$ confidence bounds. The normalisation of the model is dependent on a number of factors, including k , the ratio of energy in non-radiating particles to relativistic electrons. C10 found that k values of tens to thousands were required to bring the model normalisation into agreement with their data. Ignoring their relative normalisations, the gradient of our 235 MHz relation would agree with the model within 1.5σ , and our 1.4 GHz relation within 2.5σ .

The Willott et al. (1999) model is based on relatively straightforward synchrotron physics, but includes a number of important assumptions. The jet power is proportional to the energy density of the relativistic plasma assuming a minimum energy magnetic field, u_{me} , following the relation $P_{\text{jet}} \propto u_{\text{me}}^{3/2} \propto B_{\text{me}}^3$, where B_{me} is the minimum energy magnetic field. Willott et al. define B_{me} in terms of observable radio properties following the method given by Miley (1980), which can be simplified to $B_{\text{me}} \propto (\nu_2^{1/2-\alpha} - \nu_1^{1/2-\alpha})^{2/7}$, where ν_1 and ν_2 are frequencies defining the observable radio band (10 MHz–100 GHz for Willott et al.) and α is the spectral index. However, this assumes that the electron population in the radio-emitting plasma only contains particles with energies such that they radiate in this observable band, and Willott et al. note that the jet power will depend critically on the choice of low frequency cutoff.

Electrons with energies too low to produce observable emission may contribute a significant fraction of the energy in radio jets and lobes, since if they are present they are likely to make up the majority of the electron population. Many observational studies define the range of electron energies in terms of a range of Lorentz factors, typically with a low energy cut-off of $\gamma_{\text{min}}=10$ or 100. In a magnetic field of $\sim 1 \mu\text{G}$, such electrons will produce synchrotron radiation at $\sim 0.5\text{--}50 \text{ kHz}$, well

below the observable band. Worrall & Birkinshaw (2006) provide a relation between B_{me} and observable radio parameters using Lorentz factors rather than frequencies, which takes the form $B_{\text{me}} \propto (\gamma_{\text{max}}^{1-2\alpha} - \gamma_{\text{min}}^{1-2\alpha})^{1/(\alpha+3)}$. If we use this definition to determine u_{me} and therefore P_{jet} , the dependence of the gradient of the Willott et al. model on the spectral index becomes clear, giving a relation of the form:

$$P_{\text{jet}} \propto P_{\text{radio}}^{3/(\alpha+3)}. \quad (11)$$

This reduces to a gradient of $6/7$ for $\alpha=0.5$. However, the measured 610-235 MHz spectral indices of the G11 sample cover the range 0.53-1.44. Excluding systems for which only limits are available, the mean spectral index is $\alpha_{235}^{610} = 0.95$, implying a $P_{\text{cav}}:P_{\text{radio}}$ gradient of 0.76. This is considerably closer to our best measured gradients of ~ 0.7 for 235 MHz power and integrated radio luminosity. A spectral index of 0.8, often used as a typical value for extragalactic sources (Condon 1992) would give a model gradient of 0.79. Our best fitting $P_{\text{cav}}:L_{\text{radio}}$ relation gradient of 0.71 would suggest $\alpha \sim 1.2$.

Willott et al. developed their model to examine the relationship between low-frequency radio power and narrow line optical luminosity in a sample of 7C and 3CRR radio sources. They found no correlation between 151 MHz spectral index and the residual from their best fitting radio to optical relation. Such a correlation would be expected if jet power varied strongly with spectral index. They argue that this suggests that low-energy electrons make only a minimal contribution to jet power. However, the scatter in their dataset is large (as it is in ours) and their sample contains a wide variety of source types, for which spectral index may be dominated by emission from different physical regions. FR-II radio galaxies are also common in their sample, while our groups host only moderately powerful FR-I sources and a few FR-I/FR-II transition systems. It therefore seems possible that the slope of the relation could be steeper. Such a change in gradient may have implications for models which have used the Willott et al. relation to estimate the energy output of the population of AGN from their radio luminosity function, with a shallower gradient implying greater mechanical power available from lower luminosity jets.

3.2. Uncertainties and potential biases

Several factors could affect our estimates of the $4pV$ cavity power, or the accuracy of these estimates as a proxy for the mechanical power of the jets. These include:

- Cavity volume. Identification and characterisation of the cavity is inherently subjective, and dependent on the quality of the X-ray data, the angular and physical sizes of the cavity, its position in the group and other factors. Using HCG 62, which has several *Chandra* and *XMM-Newton* datasets with a range of exposures available, we tested the effects of performing independent spectral deprojections and having different researchers estimate cavity size. We found differences between estimates of up to a factor of 2 (~ 0.3 dex) in total cavity power, despite the relatively simple morphology of the cavities.
- Cavities at large radii are significantly more difficult to identify, owing to the decrease in X-ray intensity with radius. In both HCG 62 and NGC 5044, 235 MHz radio maps reveal lobes at large radii, beyond the cavities

identified in the X-ray (David et al. 2009; Gitti et al. 2010). In both cases there is some evidence of the presence of a cavity in the X-ray (e.g., a low abundance region suggesting multi-phase gas coincident with the detached lobe in NGC 5044 David et al. 2011), and if such cavities exist and have sizes similar to the radio lobes, this would increase our estimate of the AGN power by a factor of ~ 2 -10. Multiple cavity pairs in individual groups also give some idea of the range of cavity powers. In both NGC 5044 and NGC 5813, cavity powers for individual cavities vary by factors of up to 10.

- Very old or young cavities are unlikely to be detected. Young, small cavities would have a minimal X-ray surface brightness decrement. Their apparent cavity powers would also be small, but since they would likely be highly over-pressured, cavity power would underestimate jet power. Very old cavities would be expected to have risen to very large radii or to have already broken up into smaller structures; in either case the surface brightness decrements would be small. Their cavity powers would be low, owing to their long timescales. Non-detection of such cavities in groups could bias the $P_{\text{cav}}:P_{\text{radio}}$ relations to steeper gradients, but it is unclear how common such cavities are, or whether similar biases might also affect galaxy clusters.
- Shocks driven by the AGN outburst may contain a large fraction of the energy released. Inclusion of the shocks detected in HCG 62 and NGC 5813 (Gitti et al. 2010; Randall et al. 2011) would increase our estimate of the AGN power output by a factor ~ 10 . Given the difficulty of detecting shocks (deep *Chandra* observations are generally required) we cannot know whether we are missing a significant energy contribution in other groups.
- Uncertainties in outburst timescale will also affect power estimates. We have used the buoyancy timescale and its uncertainties when fitting the $P_{\text{cav}}:P_{\text{radio}}$ relations, and included additional error bars to show the larger uncertainty range associated with different dynamical timescale estimates, but even these may not be accurate, particularly for systems which have expanded supersonically for a significant fraction of their lifespan (e.g., UGC 408). Very old sources may also provide poor estimates if the buoyant velocity overestimates their true rate of rise; radiative ages based on synchrotron losses can exceed the dynamical timescales in such systems (e.g., in AWM 4 and NGC 507, O’Sullivan et al. 2010; Murgia et al. 2011).
- Filling factors of less than unity for radio lobes could also render volume estimates for cavities inaccurate, affecting both the energy and dynamical timescales of the outburst. Our study of AWM 4 suggested that the lobes may have a filling factor as low as $\phi=0.2$ (O’Sullivan et al. 2010).
- Jet orientation could affect our estimate of the position of cavities in the IGM, with jets close to the line of sight producing cavities which appear to be at smaller radii than is the case. This will lead to underestimates of cavity enthalpy and outburst timescale. Simulations sug-

gest that cavity powers will typically be within a factor of 3 of the true value (Mendygral et al. 2011).

- AGN-driven “weather”, turbulent motions in the IGM induced by AGN jets, could affect the position of cavities. NGC 5044 may provide an example, with several small cavities found at similar radii in the group core (David et al. 2009). Timescales for such cavities are probably underestimated, leading to overestimates of cavity power.

For our sample of groups, it appears that the effect of such biases may be to steepen the relation between cavity power and radio power. Correcting the cavity power estimates for HCG 62, NGC 5044, NGC 5813 and AWM 4 to include contributions from the probable outer cavities and shocks, and the low filling factor of the AWM 4 radio lobes, we find that the gradient of the $P_{\text{cav}}:L_{\text{radio}}$ relation flattens to 0.62 ± 0.12 . This is still consistent, within uncertainties, with our initial fit, but we note that these are perhaps the four most carefully studied systems in our sample, and deeper observations of other systems would likely lead to similar corrections. For the systems we can study in detail, corrections which reduce cavity power tend to be small, whereas the effect of including shocks and possible additional cavities can increase the estimated AGN power by much larger factors.

The impact of such biases on galaxy clusters is less clear. These are generally more X-ray luminous systems with larger cores, hosting more powerful radio sources, which might suggest that cavities will be more easily detected. The intra-cluster medium is also likely to be able to confine more powerful AGN outbursts, which in groups might simply tunnel out to large radii where any cavities would be difficult to detect (e.g., the ‘poorly-confined’ class of objects in the C10 sample). However, weak shocks may be more easily detected in galaxy groups, since the emission lines produced by gas at ~ 1 keV significantly improve our ability to accurately measure temperature. Resolution may also be a problem for more distant clusters, producing a bias toward the detection of large cavities associated with more powerful AGN outbursts. A statistical approach to the effects of such biases, based on simulations, would perhaps provide insight into this problem.

4. CONCLUSIONS

We have estimated the relations between mechanical jet power and radio luminosity, adding nine groups selected from the sample of G11 and observed with the GMRT and *Chandra* or *XMM-Newton* to the B08 sample, which consists primarily of galaxy clusters. We find $P_{\text{cav}}:P_{\text{radio}}$ relations with gradients of ~ 0.7 for both the low-frequency radio power (235 or 327 MHz) and the integrated radio luminosity, with total scatters of $\sigma_{i,L_{\text{rad}}}=0.59$ and $\sigma_{i,235}=0.58$ dex. The 1.4 GHz relation is somewhat flatter (gradient ~ 0.6) and has a slightly larger scatter, $\sigma_{i,1400}=0.65$ dex. In agreement with previous studies, this suggests that low-frequency and broad band radio measurements are superior indicators of cavity power. The weaker correlation between 1.4 GHz radio structure and the cavities identified from the X-ray makes high frequency emission a poor choice for such studies. Our fitted slopes are significantly steeper than those found by B08, but this is unsurprising since the B08 relations were determined using a different regression technique, which will tend to produce a shallower gradient. Using the same BCES orthogonal regression used for the fits to the combined dataset brings the B08 relations

into agreement with our results. Our $P_{\text{cav}}:P_{235}$ relation has a similar gradient to the $P_{\text{cav}}:P_{200-400}$ relation of C10. This is expected, given the overlap between samples, but direct comparison of the radio powers suggests that our GMRT measurements are more reliable for low-power radio galaxies.

Our $P_{\text{cav}}:P_{235}$ relation is somewhat flatter than the widely used Willott et al. (1999) model of jet mechanical and radio power, though they agree within 1.5σ uncertainties. We find that inclusion of electrons with low Lorentz factors (which cannot be directly observed) could change the gradient of the Willott model, making it dependent on the radio spectral index. In this case, using the mean spectral index of the G11 sample, the model would agree more closely with our observed relation. A variety of factors could bias or increase the uncertainty of our measurements, and we conclude that at least for galaxy groups these may have a serious impact on our cavity power estimates. Correcting for these factors, in those groups where the quality of radio and X-ray data is sufficient to allow detailed study, produces a flatter $P_{\text{cav}}:P_{\text{radio}}$ relation. However, it is unclear whether this would be the case in all groups, or in galaxy clusters, and simulations of AGN feedback across a wide range of mass scales and outburst powers are probably required to resolve this question.

We thank the anonymous referee for their useful suggestions. We thank the staff of the GMRT for their help during observations. GMRT is run by the National Centre for Radio Astrophysics of the Tata Institute of Fundamental Research. We also acknowledge support from Chandra grant AR1-12014X. EJOS thanks A. J. R. Sanderson for useful discussions and acknowledges the support of the European Community under the Marie Curie Research Training Network. SG acknowledges the support of NASA through the award of an Einstein Postdoctoral Fellowship. MG acknowledges the financial contribution from contracts ASI-INAF I/023/05/0 and I/088/06/0 and Chandra grant GO0-11136X.

REFERENCES

- Akritas, M. G., & Bershadsky, M. A. 1996, *ApJ*, 470, 706
- Best, P. N., von der Linden, A., Kauffmann, G., Heckman, T. M., & Kaiser, C. R. 2007, *MNRAS*, 379, 894
- Birzan, L., McNamara, B. R., Nulsen, P. E. J., Carilli, C. L., & Wise, M. W. 2008, *ApJ*, 686, 859, B08
- . 2010, *ApJ*, 709, 546
- Birzan, L., Rafferty, D. A., McNamara, B. R., Wise, M. W., & Nulsen, P. E. J. 2004, *ApJ*, 607, 800
- Cattaneo, A., & Best, P. N. 2009, *MNRAS*, 395, 518
- Cavagnolo, K. W., McNamara, B. R., Nulsen, P. E. J., Carilli, C. L., Jones, C., & Birzan, L. 2010, *ApJ*, 720, 1066, C10
- Churazov, E., Brüggen, M., Kaiser, C. R., Böhringer, H., & Forman, W. 2001, *ApJ*, 554, 261
- Condon, J. J. 1992, *ARA&A*, 30, 575
- Condon, J. J., Cotton, W. D., Greisen, E. W., Yin, Q. F., Perley, R. A., Taylor, G. B., & Broderick, J. J. 1998, *AJ*, 115, 1693
- David, L. P., Jones, C., Forman, W., Nulsen, P., Vrtilek, J., O'Sullivan, E., Giacintucci, S., & Raychaudhury, S. 2009, *ApJ*, 705, 624
- David, L. P., O'Sullivan, E., Jones, C., Giacintucci, S., Vrtilek, J., Raychaudhury, S., Nulsen, P. E. J., Forman, W., Sun, M., & Donahue, M. 2011, *ApJ*, 728, 162
- Dong, R., Rasmussen, J., & Mulchaey, J. S. 2010, *ApJ*, 712, 883
- Dunn, R. J. H., Allen, S. W., Taylor, G. B., Shurkin, K. F., Gentile, G., Fabian, A. C., & Reynolds, C. S. 2010, *MNRAS*, 404, 180
- Dunn, R. J. H., Fabian, A. C., & Taylor, G. B. 2005, *MNRAS*, 364, 1343
- Giacintucci, S., O'Sullivan, E., Vrtilek, J. M., David, L. P., Raychaudhury, S., Venturi, T., Athreya, R. M., Clarke, T. E., Murgia, M., Mazzotta, P., Gitti, M., Ponman, T., Ishwara-Chandra, C. H., Jones, C., & Forman, W. R. 2011, *ApJ*, accepted, arXiv:1103.1364, G11
- Giacintucci, S., Vrtilek, J. M., Murgia, M., Raychaudhury, S., O'Sullivan, E. J., Venturi, T., David, L. P., Mazzotta, P., Clarke, T. E., & Athreya, R. M. 2008, *ApJ*, 682, 186
- Gitti, M., O'Sullivan, E., Giacintucci, S., David, L. P., Vrtilek, J., Raychaudhury, S., & Nulsen, P. E. J. 2010, *ApJ*, 714, 758
- Hardcastle, M. J., Evans, D. A., & Croston, J. H. 2007, *MNRAS*, 376, 1849
- Jetha, N. N., Hardcastle, M. J., Babul, A., O'Sullivan, E., Ponman, T. J., Raychaudhury, S., & Vrtilek, J. 2008, *MNRAS*, 384, 1344
- Kaastra, J. S., Tamura, T., Peterson, J. R., Bleeker, J. A. M., Ferrigno, C., Khan, S. M., Paerels, F. B. S., Piffaretti, R., Branduardi-Raymont, G., & Böhringer, H. 2004, *A&A*, 413, 415
- Kalberla, P. M. W., Burton, W. B., Hartmann, D., Arnal, E. M., Bajaja, E., Morras, R., & Pöppel, W. G. L. 2005, *A&A*, 440, 775
- McNamara, B. R., & Nulsen, P. E. J. 2007, *ARA&A*, 45, 117
- Mendygral, P. J., O'Neill, S. M., & Jones, T. W. 2011, *ApJ*, 730, 100
- Miley, G. 1980, *ARA&A*, 18, 165
- Murgia, M., Parma, P., Mack, K., de Ruiter, H. R., Fanti, R., Govoni, F., Tarchi, A., Giacintucci, S., & Markevitch, M. 2011, *A&A*, 526, A148+
- O'Sullivan, E., Giacintucci, S., David, L. P., Vrtilek, J. M., & Raychaudhury, S. 2010, *MNRAS*, 868
- Peterson, J. R., & Fabian, A. C. 2006, *Phys. Rep.*, 427, 1
- Peterson, J. R., Kahn, S. M., Paerels, F. B. S., Kaastra, J. S., Tamura, T., Bleeker, J. A. M., Ferrigno, C., & Jernigan, J. G. 2003, *ApJ*, 590, 207
- Pratt, G. W., Croston, J. H., Arnaud, M., & Böhringer, H. 2009, *A&A*, 498, 361
- Rafferty, D. A., McNamara, B. R., Nulsen, P. E. J., & Wise, M. W. 2006, *ApJ*, 652, 216
- Randall, S. W., Forman, W. R., Giacintucci, S., Nulsen, P. E. J., Sun, M., Jones, C., Churazov, E., David, L. P., Kraft, R., Donahue, M., Blanton, E. L., Simionescu, A., & Werner, N. 2011, *ApJ*, 726, 86
- Randall, S. W., Jones, C., Kraft, R., Forman, W. R., & O'Sullivan, E. 2009, *ApJ*, 696, 1431
- Sanderson, A. J. R., Ponman, T. J., & O'Sullivan, E. 2006, *MNRAS*, 372, 1496
- Smith, R. K., Brickhouse, N. S., Liedahl, D. A., & Raymond, J. C. 2001, *ApJ*, 556, L91
- Verkhodanov, O. V., Trushkin, S. A., Andernach, H., & Chernenkov, V. N. 1997, in *Astronomical Society of the Pacific Conference Series*, Vol. 125, *Astronomical Data Analysis Software and Systems VI*, ed. G. Hunt & H. Payne, 322
- Willott, C. J., Rawlings, S., Blundell, K. M., & Lacy, M. 1999, *MNRAS*, 309, 1017
- Worrall, D. M., & Birkinshaw, M. 2006, in *Lecture Notes in Physics*, Berlin Springer Verlag, Vol. 693, *Physics of Active Galactic Nuclei at all Scales*, ed. D. Alloin, 39